Magnetoelastic mechanism of long-range magnetic ordering in magnetic/nonmagnetic multilayers

Helen Gomonay
National Technical University of Ukraine "KPI," 37, ave Peremogy, 03056, Kyiv, Ukraine
(Received 25 September 2000; revised manuscript received 13 February 2001; published 2 July 2001)

The observed correlation in antiferromagnetic (AFM) ordering across a nonmagnetic spacer is interpreted in the framework of the phenomenological model. It is shown that the magnetostriction of one magnetically ordered layer produces a strain field of the same symmetry in the next magnetic layer via the spacer. Such an induced anisotropy favors a correlated orientation of the magnetic moments in all the layers. The value of the induced anisotropy is proportional to the magnetostriction constant and it exponentially decreases with an increase of the spacer thickness. A corresponding short-range interaction gives rise to an ordering of the AFM layers throughout the film thickness and reveals itself in a linewidth of neutron diffraction spectra. Theoretical predictions are in satisfactory agreement with the available experimental data.

DOI: 10.1103/PhysRevB.64.054404 PACS number(s): 75.70.−i, 75.50.Ee

I. INTRODUCTION

The phenomenon of interlayer coupling in artificially grown superlattices consisting of alternating magnetic and nonmagnetic layers is a matter of great concern from both a fundamental and theoretical point of view. In metal-based multilayers (ML's) the magnetic ordering is transferred over the nonmagnetic spacer due to the presence of long-range RKKY interactions. A different situation arises in semiconductors with low carrier density, especially in the ML's made of antiferromagnetic (AFM) materials. Of special interest among these systems are the AFM multilayers produced on the basis of Mn chalcogenides and zinc-blende II-VI semiconductors and also the (111) EuTe/PbTe system with a rather thin (up to 10–15 monolayers) nonmagnetic spacer.

The MnTe-based films grown by molecular beam epitaxy have been widely studied experimentally.[1–11] The Mn chalcohenides alloyed with nonmagnetic II-VI compounds (e.g., CdTe, ZnTe, ZnSe, etc.) crystallize into zinc-blende structure and give a peculiar example of a frustrated fcc antiferromagnet with the Mn-Mn exchange coupling limited to a few nearest coordination spheres.[1,12] On the contrary, epitaxial films of MnTe– and MnTe-based ML's show long-range AFM-III type ordering that is inspired by the large strains produced by the mismatch between the lattice parameters of the substrate and film and also of the magnetic and nonmagnetic layers. However, in the ML structure the AFM ordering is usually locked inside the MnTe layer. While the correlation length inside the layer ranges to 1000 Å in the film plane,[1] no interlayer correlation was detected for a nonmagnetic spacer width larger than 15 monolayers. So it was quite surprising when the elastic neutron scattering measurements of the ML's of different composition [MnTe/CdTe (Refs. 2 and 4) and (Refs. 6–10)] MnTe/ZnTe revealed the coherence in AFM spin ordering that extended across multiple (up to seven) bilayers through the relatively thick (up to 30 Å) nonmagnetic spacer. In the canted structures in MnTe/CdTe films with an ultrathin nonmagnetic spacer (the nonmagnetic/AFM ratio being 2:7, 2:10, 4:9, 6:10) the correlation concerned not only the orientation and pitch of the AFM helices in neighboring MnTe layers, but also the phase of the helix.[4] In Refs. 7–9 the same correlation was observed in the MnTe/ZnTe structure with an AFM/nonmagnetic monolayer ratio of $20{:}m$ and $10{:}m$ ($m=4-10$) in a wide temperature interval. The crucial enhancement of the correlation length was observed in the Cl-doped MnTe/ZnTe ML.[10] The transfer of the magnetic excitations through the nonmagnetic buffer deduced from the magnon spectra for MnTe/ZnTe multilayer[6] also indicates the presence of strong interlayer coupling. In all experiments mentioned the estimated coherence length across the layers was greater than 30 Å.

A very similar effect of the unusually strong interlayer coupling over the nonmagnetic spacer was observed in the (111) EuTe/PbTe ML.[13–17] For this system the AFM ordering was still detected even for a spacer thickness of 55 Å .[14] The AFM-II type structure of EuTe consists of alternating ferromagnetically ordered (111) planes which are coupled antiferromagnetically to each other. In the case of an even number of sheets in the EuTe layer, the layer is pure AFM, whereas for an odd number of sheets it is effectively ferrimagnetic. The experiments[14] have shown the most pronounced correlation for the case of a four-sheet (pure AFM) EuTe layer, for which the dipolar mechanism of the interlayer coupling should be excluded.

The reason for so long a range of magnetic correlation across the nonmagnetic spacer is still unclear. The superexchange interactions between Mn and exchange interactions between Eu^{2+} spins are short range and could not cover the 30 Å distance. Also, the magnetic interactions could not be transferred by the RKKY mechanism, because the nonmagnetic Te-based semiconductors (CdTe, ZnTe, PbTe) possess too few carriers compared with the metals.[4,14,16]

The possible explanation for the phenomena discussed may be based on the magnetoelastic mechanism. MnTe-based compounds show a considerable magnetostriction (shear strain attains 0.3%) observed at the Néel point.[3,5] The AFM structure of the MnTe-based and EuTe/PbTe ML's can be realized in the form of different orientational domains characterized by mutually noncollinear AFM vectors. So orientational degeneracy of the AFM state and strong magnetoelastic interactions make it possible to consider the long-range elastic forces as being responsible for the correlation in spin ordering in neighboring magnetic layers.[18]

In the present paper I develop the phenomenological model that interprets the interlayer magnetic coupling across the nonmagnetic spacers in semiconductor ML's as resulting from the magnetoelastic interactions.

II. MAGNETIC STRUCTURE OF THE BULK EPILAYER

The crystal structure of the thick (1 μm) MnTe film is described by the $F\bar{4}3m$ space group. The magnetic structure is rather complicated and corresponds to a pure AFM-III structure.[1] The phase transition into the AFM structure is described with a six-armed star $\mathbf{k}_8$ (in Kovalev's notation[20].) The corresponding magnetic and magnetoelastic contribution to the free energy density is given by

$$f_{\mathrm{me}}=\frac{1}{2}\beta[M_x^2(\mathbf{q}_1)+M_y^2(\mathbf{q}_1)+M_y^2(\mathbf{q}_2)+M_z^2(\mathbf{q}_2)+M_z^2(\mathbf{q}_3)+M_x^2(\mathbf{q}_3)]+\lambda_1\{[M_x^2(\mathbf{q}_1)+M_y^2(\mathbf{q}_1)](2u_{zz}-u_{xx}-u_{yy})+[M_y^2(\mathbf{q}_2)+M_z^2(\mathbf{q}_2)](2u_{xx}-u_{yy}-u_{zz})+[M_z^2(\mathbf{q}_3)+M_x^2(\mathbf{q}_3)](2u_{yy}-u_{zz}-u_{xx})\}+\lambda_2\{[M_x^2(\mathbf{q}_1)-M_y^2(\mathbf{q}_1)](u_{xx}-u_{yy})+[M_y^2(\mathbf{q}_2)-M_z^2(\mathbf{q}_2)](u_{yy}-u_{zz})+[M_z^2(\mathbf{q}_3)-M_x^2(\mathbf{q}_3)](u_{zz}-u_{xx})\}, \tag{1}$$

where $\mathbf{M}(\mathbf{q}_i)$, $i=1, 2, 3$, are the magnetic order parameters, corresponding to different arms of the $\mathbf{k}_8$ star. The vectors $\mathbf{q}_1=(2\pi/a,0,\pi/a)$, $\mathbf{q}_2=(\pi/a,2\pi/a,0)$, $\mathbf{q}_3=(0,\pi/a,2\pi/a)$ may be associated with the direction in which the unit cell is multiplied in the course of AFM phase transitions. Three other equivalent arms that generate so-called translational domains are omitted. The strain tensor components u_{ij} are attributed to the cubic crystal axes. In the magnetic energy I hold only the second-order magnetic anisotropy constant β, and $\lambda_{1,2}$ are responsible for the magnetoelastic interactions.

AFM ordering in the bulk sample can occur in the form of either collinear (as in MnTe/ZnTe) or canted (Keffer) (as in MnTe/CdTe) AFM-III structure.[1] The order parameter of the collinear structure is one of the $\mathbf{M}(\mathbf{q}_i)$ component. Correspondingly, the structure can be materialized in the six types of orientational domains, related to three different $\mathbf{q}_i$ and two possible components of $\mathbf{M}$ vector. In the canted structure both $\mathbf{M}$ components are equally represented, e.g., $M_x(\mathbf{q}_1)=M_y(\mathbf{q}_1)$, and three types of the orientational domains could be observed.

In the multilayered structure the effect of lattice distortion on the magnetic and nonmagnetic layers partially removes the degeneracy of the domain structure. If the film axis is oriented along the z direction, then in the paramagnetic phase (over the Néel point) the equilibrium strain tensor of the magnetic layers has tetragonal symmetry,

$$u_{xx}^0=u_{yy}^0=\epsilon_1, \quad u_{zz}^0=\epsilon_2, \tag{2}$$

and the anisotropy energy is renormalized as follows:

$$f_{\mathrm{an}}=\frac{1}{2}[\beta+4\lambda_1(\epsilon_2-\epsilon_1)][M_x^2(\mathbf{q}_1)+M_y^2(\mathbf{q}_1)]+\frac{1}{2}[\beta-2\lambda_1(\epsilon_2-\epsilon_1)][M_y^2(\mathbf{q}_2)+M_z^2(\mathbf{q}_2)+M_z^2(\mathbf{q}_3)+M_x^2(\mathbf{q}_3)]+\lambda_2(\epsilon_1-\epsilon_2)[M_y^2(\mathbf{q}_2)-M_z^2(\mathbf{q}_2)+M_x^2(\mathbf{q}_3)-M_z^2(\mathbf{q}_3)], \tag{3}$$

The values $\epsilon_{1,2}$ are the misfit strains in and perpendicular to the film plane, respectively.

From Eq. (3) it follows that for the AFM–III collinear structure the number of equivalent orientational domains is reduced to 2 and for AFM-III canted structure to 1 if $\lambda_1(\epsilon_2-\epsilon_1)<0$ and, correspondingly, to 4 and 2 in the opposite case. Hereafter we will consider the first case with $\lambda_1(\epsilon_2-\epsilon_1)<0$, which corresponds to the two-times-degenerated collinear structure with multiplication of the unit cell in the z direction and $M_x(\mathbf{q}_1)=M_0$, $M_y(\mathbf{q}_1)=M_z(\mathbf{q}_1)=0$ (A-type domain) or $M_y(\mathbf{q}_1)=M_0$, $M_x(\mathbf{q}_1)=M_z(\mathbf{q}_1)=0$ (B-type domain). The other cases can be treated in a similar way.

III. FORMATION OF THE DOMAIN STRUCTURE INSIDE THE AFM LAYER

AFM ordering results in the appearance of additional strains in the magnetic layers, $u^{(\mathrm{ms})}$, that are different in the different orientational AFM domains. As a result of the rather large value of the magnetoelastic constants, this degeneracy influences greatly the formation of the domain structure in the whole sample. To describe the formation of the domain structure in a single AFM layer we should take into account the fact that in equilibrium the average macroscopic strains, $\langle u_{xx}^{(\mathrm{ms})}\rangle$, $\langle u_{yy}^{(\mathrm{ms})}\rangle$, and $\langle u_{xy}^{(\mathrm{ms})}\rangle$ (brackets mean averaging over the xy plane) should vanish. This can be accounted for by introducing the following term into the free energy density:

$$f_{\mathrm{stray}}=\frac{1}{2}[\alpha_1\langle u_{xx}^{(\mathrm{ms})}-u_{yy}^{(\mathrm{ms})}\rangle^2+4\alpha_2\langle u_{xy}^{(\mathrm{ms})}\rangle^2], \tag{4}$$

where the coefficients $\alpha_{1,2}$ in neglect of small surface effects can be expressed through the shear elastic moduli of the cubic phase: $\alpha_1=c_{11}-c_{12}$, $\alpha_2=c_{44}$. This energy is analogous to the stray (magnetostatic) energy in ferromagnets. It originates from the compatibility conditions between the phases with different spontaneous strains (in our case, these are the AFM and nonmagnetic layers). Calculation of this expression is given in the Appendix. The domain distribution in the xy plane can be then found from the minimization of a free energy density per layer thickness:

$$F_{\mathrm{layer}}=\int\int_S dxdy(f_{\mathrm{me}}+f_{\mathrm{e}})+Sf_{\mathrm{stray}}, \tag{5}$$

where the stray energy is given by Eq. (4), averaging, and integration is implied over the surface of the layer, S. The term

$$f_{\mathrm{me}}=\lambda_2 M_0^2[u_{xx}^{(\mathrm{ms})}-u_{yy}^{(\mathrm{ms})}]\rho(x,y) \tag{6}$$

is the principal contribution to the magnetoelastic energy (1) with account of two types of orientational domains A and B; M_0, as was already mentioned, is the value of sublattice magnetization. In Eq. (6) I have introduced an Ising-type variable that specifies the type of domain:

$$\rho(x,y)=\begin{cases} 1, & \text{in the A domain,} \\ -1, & \text{in the B domain.} \end{cases}$$

The elastic energy of the sample is expressed in a standard way:

$$f_{\mathrm{e}}=\frac{1}{2}u_{ij}c_{ijkl}u_{kl}, \tag{7}$$

where $\hat{\hat{c}}$ is the tensor of elastic moduli corresponding to the cubic crystal symmetry.

From minimization of Eq. (5) it follows that A and B domains should be distributed in the xy plane with an equal probability. The size of the domains, R, can be estimated from the balance of the interface (AFM/nonmagnetic phase) energy and the energy of the domain boundaries. The interface energy grows linearly with R, while the domain boundary contribution decreases as $1/R$, so there is an optimal shape-dependent size R_{opt}. A rough evaluation[21] gives $R_{\mathrm{opt}} \propto a/2u^{(\mathrm{ms})} \propto 1000$ Å (where $a \propto 6.3$ Å is the lattice parameter), which correlates with the experimental data[1,3,4] which reveal the presence of the temperature-dependent AFM domain structure in the thick MnTe epilayers, the size of the domains being of the order of 1000 Å.

In the ML the size of the AFM domain can be also influenced by the distribution of the microstresses produced in the course of film growth. In this case $u^{(\mathrm{ms})}$ should be substituted by the characteristic misfit strain $u^{(\mathrm{misfit})}$ that can reach up to 6%.[1] In this case the domain size is diminished down to 50 Å.

IV. INTERACTION THROUGH THE NONMAGNETIC SPACER

From the general point of view, an interlayer coupling may be explained as follows. In a perfect lattice the magnetic layers are elastically conjugated with the adjacent nonmagnetic spacers due to compatibility conditions. So magnetostriction of one magnetically ordered layer produces a strain field of the same symmetry in the next magnetic layer via the spacer. Such an induced anisotropy favors a parallel orientation of the magnetic moments in all layers. In fact, if the neighboring AFM layers fit in the same domain type, the nonmagnetic spacer, sandwiched in between, will undergo the same stress (tension or compression) from both sides. In the case when the AFM layers belong to different domain types, the nonmagnetic spacer will undergo tension from one side and compressive stress from the other one. Thus, in the first case the magnetostriction causes homogeneous while in the second case inhomogeneous strains. It seems reasonable to assume that the configuration with a homogeneous strain distribution is more favorable.

The value of the induced stress and strain field is obviously proportional to the magnetostriction constant and it should decrease with an increase of the spacer thickness. To calculate this field and interaction energy between the different AFM layers, let us consider the following model.

(i) We assume that the tensor of the elastic moduli of the ML film is homogeneous (nonhomogeneity of the elastic modula arises from nonlinear elastic effects and, far from the points of structural phase transitions, can be neglected).

(ii) We consider the region in the form of a z-oriented cylinder with the radius $R/2$ in the xy plane. With the assumption that R corresponds to the domain size in the xy plane, the AFM structure is homogeneous (monodomain) inside the layer.

(iii) We suppose that a local magnetic order has been already established.

So the question that we are going to answer is, are the adjacent AFM layers ordered in the same way (say, A and A domains) or in a different way (A and B domains)? To answer this question, one should start from the following expression for the free energy of the described cylinder:

$$F=\int dV\left\{ f_{\mathrm{e}}+\sum_n f_{\mathrm{me}}^{(n)}\theta_n \right\}, \tag{8}$$

where elastic energy f_{e} is given by Eq. (7). Periodical alteration of the magnetic and nonmagnetic layers is described by a form function

$$\theta_n(z)=\begin{cases} 1, & Dn-d/2<z<Dn+d/2, \\ -1, & Dn+d/2<z<D(n+1)-d/2, \end{cases} \tag{9}$$

where D is the period of the structure, d is the thickness of the AFM layer, $n=1,\ldots,N$ is the number of bilayers, and N is the whole number of the bilayers in the film. The expression for magnetoelastic energy is analogous to Eq. (6):

$$f_{\mathrm{me}}^{(n)}=\lambda_2 M_0^2[u_{xx}^{(\mathrm{ms})}-u_{yy}^{(\mathrm{ms})}]\rho_n, \tag{10}$$

where the Ising variable

$$\rho_n=\begin{cases} 1, & \text{if the } n\text{th layer is of the A type,} \\ -1, & \text{if the } n\text{th layer is of the B type,} \end{cases}$$

depends upon the number of AFM layers.

Standard equilibrium conditions for the elastic media have a form[22]

$$\frac{\delta F}{\delta \mathbf{u}}=0, \tag{11}$$

where $\mathbf{u}$ is a shift vector. Equation (11) for the equilibrium continuous functions $\mathbf{u}(\mathbf{r})$ can be easily solved with the help of a Fourrier transformation; the corresponding components $\mathbf{u}(\mathbf{k})$ are found as follows:

$$\mathbf{u}(\mathbf{k}) = \imath\lambda_2 M_0^2 \hat{G}(\mathbf{k}) \begin{pmatrix} k_x \\ -k_y \\ 0 \end{pmatrix} \sum_n \rho_n \theta_n(\mathbf{k}), \tag{12}$$

where $\hat{G}^{-1}(\mathbf{k}) = \hat{\hat{c}}\mathbf{kk}$ is a dynamic matrix, and $\theta_n(\mathbf{k})$ is a Fourier transform of $\theta_n(z)$. Substituting Eq. (12) into Eq. (8), one obtains the following expression for the equilibrium elastic energy contribution for a given magnetic ordering:

$$F = -V\frac{\lambda_2^2 M_0^4(T)}{2c_{44}}\left[\left(\frac{d}{DN}\sum_m \rho_m\right)^2 + \frac{R}{2ND}\sum_{0<n<m} I_n \rho_{n+m}\rho_m\right], \tag{13}$$

where V is the crystal volume, and c_{44} is the shear modulus. Expression (13) contains positive interaction constants

$$I_n = K\exp\left(-\frac{2\xi_1 Dn}{R}\right)\sinh^2\left(\frac{\xi_1 d}{R}\right)\frac{5c_{11}+3c_{44}}{8c_{11}} > 0, \tag{14}$$

where $\xi = 5.13$ is the first zero of the Bessel function J_2, and $K = 3.3\times 10^{-3}$ is a numerical constant. [In the expression (13) I have assumed that the elastic properties of the film with the initially cubic lattice are isotropic, i.e., $c_{11} - c_{12} = 2c_{44}$.] The first term in Eq. (13) arises from the homogeneous strains, the second one reflects the constraints imposed by the compatibility conditions for the elastic strains [continuity of the shift vector $\mathbf{u}(\mathbf{r})$]. The main conclusion that can be drawn from Eq. (13) is the following. If in the nth and mth layers the AFM structure is the same (both A-A or both B-B domains), then $\rho_m\rho_n = 1$, and the corresponding term in Eq. (13) would be negative and thus would reduce the energy. In the opposite case of different domains $\rho_m\rho_n = -1$, and the corresponding contribution will be positive (so in this case the energy increases). The value of the interaction constant (14) exponentially decreases with the width of the nonmagnetic spacer, so the main contribution to Eq. (13) arises from the adjacent AFM layers. Because of the positiveness of this constant, ''ferromagnetic'' ordering of the AFM domains is more favorable. So magnetoelastic interactions establish the correlation between the AFM structure in different layers.

V. DISTRIBUTION OF THE AFM DOMAINS OVER DIFFERENT MAGNETIC LAYERS

The model developed above shows the presence of the elastically induced long-range ordering [first term in Eq. (13)] and short-range correlation [second term in Eq. (13)] between the orientation of the AFM vectors in the different magnetic layers separated by the nonmagnetic spacer. Quantitatively long-range order is characterized by the order parameter ρ (thermodynamic average of ρ_n, $\langle\rho_n\rangle_T$), and short-range order is characterized by the correlation function $\Gamma_m = \langle\rho_n\rho_{n+m}\rangle_T - \langle\rho_n\rangle_T^2$; both values can be calculated with the use of the well-known[24] results for the one-dimensional (1D) Ising model with energy density (per bilayer volume)

$$f = -H_{\text{eff}}\sum_m \rho_m - J\sum_m \rho_m\rho_{m+1}, \tag{15}$$

where the effective mean field results from the first (long-range) term in Eq. (13),

$$H_{\text{eff}} = \frac{\lambda_2^2 M_0^4(T)}{2c_{44}}\frac{d^2}{D^2}\rho, \tag{16}$$

and I have neglected all but the greatest interaction coefficient in the second sum in Eq. (13):

$$J = \frac{\lambda_2^2 M_0^4(T)}{2c_{44}}\frac{R}{2D}I_1. \tag{17}$$

The effective field (16) stabilizes the long-range ordering of the AFM domains, and corresponding parameter is given implicitly by the equation

$$\rho = \tanh\frac{H_{\text{eff}}(\rho)}{T}, \tag{18}$$

where T is the temperature. The correlation function can be calculated using the matrix technique (see Ref. 24 for details). The ultimate expression in the limit of large $N\to\infty$ is the following:

$$\Gamma_m = \frac{2\rho^2(1-\rho^2)\sinh(2J/T)}{e^{-2J/T}+2\rho^2\sinh(2J/T)} + \frac{(1-\rho^2)\omega^m}{e^{-2J/T}+2\rho^2\sinh(2J/T)}, \tag{19}$$

where ρ is defined by Eq. (18) and

$$\omega = \frac{\rho^2+\coth(2J/T)}{1-\rho^2} - \frac{\sqrt{1+2e^{2J/T}\rho^2\sinh(2J/T)}}{(1-\rho^2)\sinh(2J/T)}. \tag{20}$$

At low temperature, $\rho\to 1$, $J/T\to\infty$, and Γ_m tends to 0, which reflects the tendency to long-range ordering with infinite correlation length. The short-range contribution to the correlation length is important at high temperature, where $J/T \ll 1$. For this region

$$\Gamma_m = (J/T)^m, \tag{21}$$

where I supposed that $\rho \ll 1$. The Fourrier image of Γ_m,

$$\Delta(q) = \sum_m \Gamma_m \exp(\imath mqD) = \frac{1-(J/T)\cos(qD)}{1+J/T-2(J/T)\cos(qD)} \approx \frac{1-J/T}{1-J/T+J/T(qD)^2}, \tag{22}$$

gives rise to a Lorentz-shape dependence versus wave vector q. It can be associated directly with the neutron diffraction spectrum. The corresponding correlation length which characterizes the Lorentz-peak width is found from analysis of the denominator in Eq. (22):

$$\kappa = D\sqrt{\frac{J/T}{1-J/T}}. \tag{23}$$

If we substitute Eqs. (14) and (17) into Eq. (23) and suppose that the nonmagnetic spacer is much thinner than the AFM one, $(D-d) \ll D,d$, then,

$$\kappa \propto \sqrt{DR}\frac{M_0^2(T)}{\sqrt{T}}\exp\left(-\frac{\xi_1(D-d)}{R}\right). \tag{24}$$

So the correlation length exponentially decays with the width of the nonmagnetic spacer and decreases with temperature growth due to the magnetostriction decrease [factor $M_0(T)$] and thermal fluctuations (denominator $\sqrt{T}$).

VI. DISCUSSION

The results of the previous sections make it possible to deduce that (1) the superlattices with intermediately thick nonmagnetic spacer should show the long-range ordering of the AFM domains in the direction of the film normal. This effect should reveal itself in a system of magnetic Bragg peaks corresponding to the superlattice period. (2) The correlation length, i.e., the characteristic distance at which the AFM layers belong to the same domain type, exponentially decays with nonmagnetic spacer width. (3) Close to the Néel point, the long-range ordering should vanish, and the domains of both types should be equally represented not only in the xy plane, but also in the z direction.

The appropriateness of this model may be analyzed on the basis of neutron diffraction data for MnTe/ZnTe (Refs. 7,8, and 10) and (111) EuTe/PbTe (Refs. 13–15). The scans of the neutron scattering intensity at the (0,1,1/2) AFM reflections for $(MnTe)_{10}(ZnTe)_5$ and $(MnTe)_{20}(ZnTe)_4$ (Ref. 8) reveal a fundamental magnetic peak along with harmonic sidebands. At 10 K the main peak is rather narrow and the separation between the peaks corresponds to the superlattice period D, which points to the presence of long-range ordering in the growth direction. The width of the principal peak decreases exponentially versus the nonmagnetic spacer width as can be seen from Fig. 1. This figure shows the experimental data taken at 10 K (Refs. 7 and 8) for the $(MnTe)_{10}(ZnTe)_x$ (circles) and $(MnTe)_{20}(ZnTe)_x$ (squares) along with the theoretical curves calculated from Eq. (24) with $R=56$ Å for $(MnTe)_{10}(ZnTe)_x$ and $R=28$ Å for $(MnTe)_{20}(ZnTe)_x$. The adjustment parameter R may be treated, as was mentioned above, as a domain size in the xy plane. The small value of R is in agreement with an extremely small thickness of the domain walls x_0 separating the different AFM domains. The magnitude of x_0 is usually evaluated as the square root of the exchange to the in-plane anisotropy ratio. The exchange constant as deduced from the Néel temperature[8] (75 K) is $\propto 4.1\times a^2$ MJ/m (where a is the lattice constant); the in-plane strain-induced anisotropy, according to Eq. (3), is $\propto \lambda M_0^2(\epsilon_2-\epsilon_1)=2.4$ MJ/m^3. [The magnetoelastic constant was calculated as $\lambda M_0^2 \propto 2c_{44}u^{(ms)} = 55$ MJ/m^3 from a typical magnitude of the shear modulus $2c_{44}=182$ MJ/m^3 (see Ref. 25) and that of spontaneous magnetostriction for the MnTe epilayer $u^{(ms)}=0.3\%$ (see Ref. 1); $\epsilon_2-\epsilon_1=5\%$ is associated with the misfit strain.] So rather close values of the exchange and anisotropy constants give rise to an atomically sharp domain wall with thickness $x_0 \propto 1.3a \propto 8$ Å.

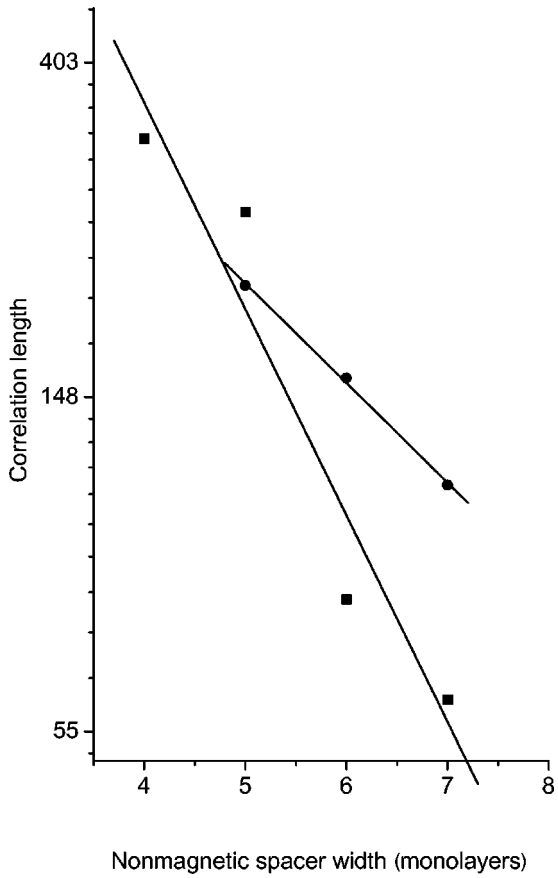

FIG. 1. Correlation length vs nonmagnetic spacer width for MnTe/ZnTe multilayers at $T=10$ K plotted in logarithmic scale. Taken from the scan of the magnetic peak (1, 0, 0.5) along [001] (Ref. 8). Circles correspond to 10 monolayers of MnTe, squares to 20 monolayers. Solid lines: theoretical approximation (see text for details).

Another peculiar feature—the dependence of R on the thickness of the AFM slab—correlates with the rough evaluation made in Sec. III. Really, the magnetostriction value inside the AFM layer depends upon the ratio between the AFM and nonmagnetic parts. The larger the AFM layer, the greater the strain and, correspondingly, the in-plane domain size R diminishes.

Extrapolation of the obtained κ vs $(D-d)$ dependences toward small (below 2 ML) and large (over 10 ML) values of the nonmagnetic spacer width shows that for an extremely small spacer $(d \to D)$ the correlation length becomes comparable with the sample thickness [nearly 0.4 μm for $(MnTe)_{20}(ZnTe)_x$ ML's and 0.13 μm for $(MnTe)_{10}(ZnTe)_x$ ML's]. This means almost perfect long-range ordering, which can be associated with the presence of the elastic mean field H_{eff} [see Eq. (16)]. In the limit of a large spacer, the correlation length falls down to 11 Å for $(MnTe)_{20}(ZnTe)_x$ and to 42 Å for $(MnTe)_{10}(ZnTe)_x$,

which means no correlation for a spacer 12 and greater ML thick.

The analysis of the diffraction data for MnTe/ZnTe taken at different temperatures[7,8,10] exhibits a spreading of the principal peak with the temperature growth in accordance with the fluctuation-induced decay of the correlation [see Eq. (24)]. Close to the Néel temperature this peak is entirely replaced by a new set of symmetrically shifted satellites that are located approximately midway between the superlattice harmonics. The imprints of the ''double-period'' peaks can be traced even at 10 K. These satellites may be attributed to randomly distributed domains of both types, the position of the peaks being associated with the presence of ''superstructural domain walls,'' i.e., the pairs of neighboring bilayers containing domains of opposite (A and B) type.

Demolition of long-range ordering at low temperature is associated with the rotation of all spins in an AFM layer over the hard magnetization axis. In this region the simple 1D model developed in Sec. V should be completed in view of the necessity for spins to overcome the potential barrier. Rigorous calculations are out of scope of this paper, and I restrict myself to an approximate evaluation of the characteristic temperature for the break of the AFM domain structure. The potential barrier established by the in-plane anisotropy is of the order of 2.4 MJ/m^3 (see the discussion above), which corresponds to 44 K, and this value correlates well with the temperature at which the intensities of the main peak and ''double-period'' satellites became equal.[8]

Neutron diffraction data on (111) EuTe(4)/PbTe(12) ML (Refs. 13–15) taken at 4.2 K (the Néel temperature is 9.6 K) also show a set of pronounced peaks corresponding to long-range correlation in AFM ordering in the growth direction. This correlation is still preserved even if the sample was cooled down in an external magnetic field (<0.5 T) applied in the film plane in the $[1\bar{1}0]$ direction.[14,16] We can assume that the higher magnetic field produces additional magnetostriction and thus inhibits weak interlayer coupling and destroys the long-range ordering across the film.[25]

The model developed suggests a possible, magnetoelastic, mechanism of interlayer coupling that supposedly can be the only one for the case of perfect interfaces, intermediate (4–8 ML) spacer thicknesses, and low-impurity ($<10^{17}$ cm^{-3}) and carrier concentration. Small thicknesses of 1–2 ML are enough to ensure exchange interactions, impurities provide a kind of superexchange through hydrogenic states, as was shown in Ref. 26, and interface roughness reduces mismatch stresses and may serve as a source of ferromagnetic charges that result in long-range dipole-dipole interactions between the layers.

VII. SUMMARY AND CONCLUSIONS

(i) Long-range magnetoelastic interactions between magnetic and nonmagnetic phases result in the appearance of domain structure in the film plane.

(ii) The observed interlayer coupling via the nonmagnetic spacer can be due to long-range elastic interactions. These interactions tend to align AFM moments in different layers in parallel.

(iii) Interlayer correlation reveals itself in the thinning of the magnetic peaks with a decrease of temperature and nonmagnetic spacer width. Temperature-induced demolition of the interlayer coupling gives rise to the occurrence of domains of different types, which is observed as additional magnetic peaks shifted from the ideal (0, 1, 1/2) position. These predictions are in good agreement with the available experimental data.

(iv) The model developed with a slight modification can be applied for a description of the phase and pitch correlation in canted AFM structures in MnTe/CdTe ML's and also to AFM-II (111)EuTe/PbTe ML's. The same mechanism can also be responsible for the transport of spin excitations observed in Ref. 6.

ACKNOWLEDGMENTS

I am grateful to Professor W. Szuszkiewicz for the valuable discussions and unpublished materials kindly provided. I also would like to acknowledge Professor S. M. Ryabchenko for the idea of the paper, and A. A. Malyshenko for financial and technical support. Special acknowledgment goes to Professor J. Kirschner for fruitful discussions and the opportunity to revise the paper using the facilities of MPI Halle (Saale), Germany.

APPENDIX: CALCULATION OF THE STRAY ENERGY

Let us consider an AFM layer constrained between two nonmagnetic layers. Above the Néel temperature the structure is relaxed and can be treated as nonstressed and zero strained. Spontaneous strains $\hat{u}$ that occur below the Néel temperature should satisfy the compatibility conditions at the AFM/nonmagnetic interface, which can be written as follows:

$$\mathbf{N}\times\hat{u}(\mathbf{r_S})\times\mathbf{N}=0, \tag{A1}$$

where $\mathbf{N}$ is an interface normal. The equilibrium strain can be represented as a sum of self-magnetostriction $\hat{u}^{(\mathrm{ms})}(\mathbf{r})$ (in principle, inhomogeneous one), which satisfies the compatibility conditions $\mathrm{inc}\hat{u}^{(\mathrm{ms})}\equiv-\mathrm{rotrot}\hat{u}^{(\mathrm{ms})}(\mathbf{r})=0$ and extra strain $\hat{u}^{(\mathrm{add})}(\mathbf{r})$:

$$\hat{u}(\mathbf{r})=\hat{u}^{(\mathrm{ms})}(\mathbf{r})+\hat{u}^{(\mathrm{add})}(\mathbf{r}). \tag{A2}$$

The last term in Eq. (A2) can be treated as an additional strain field induced by the ''interface incompatibility charges''

$$\hat{\eta}(\mathbf{r})=-\delta'[(\mathbf{r}-\mathbf{r}_S)\mathbf{N}]\mathbf{N}\times\hat{u}^{(\mathrm{ms})}(\mathbf{r}_S)\times\mathbf{N}, \tag{A3}$$

where δ is Dirac's delta function, and the prime means a derivative versus an argument. The function $\hat{u}^{(\mathrm{add})}(\mathbf{r})$ can be found explicitly from the equation

$$\mathrm{inc}\hat{u}^{(\mathrm{add})}(\mathbf{r})=\hat{\eta}(\mathbf{r}) \tag{A4}$$

as follows (for details see Ref. 27):

$$\hat{u}^{(\mathrm{add})}(\mathbf{r}) = \frac{1}{4\pi}\int_{\Omega} dV' \frac{\hat{\eta}(\mathbf{r}') - \hat{1}\ \mathrm{Tr}\ \hat{\eta}(\mathbf{r}')}{|(\mathbf{r}-\mathbf{r}_S)|}$$

$$= \frac{1}{4\pi}\int_{S} dS \frac{(\mathbf{N},\mathbf{r}-\mathbf{r}_S)}{|(\mathbf{r}-\mathbf{r}_S)|^3}\hat{q}(\mathbf{r}_S), \qquad \text{(A5)}$$

where

$$\hat{q} \equiv \hat{u}^{(\mathrm{ms})} + \mathbf{N}\otimes\mathbf{N}\,\mathrm{Tr}\,\hat{u}^{(\mathrm{ms})} - \mathbf{N}\otimes(\hat{u}^{(\mathrm{ms})}\mathbf{N}) - (\hat{u}^{(\mathrm{ms})}\mathbf{N})\otimes\mathbf{N}.$$

The strains $\hat{u}^{(\mathrm{add})}(\mathbf{r})$ produce the "twinning" stresses

$$\hat{\sigma} = \hat{\hat{c}}\hat{u}^{(\mathrm{add})}, \qquad \text{(A6)}$$

analogous to a demagnetization field in ferromagnets. In Eq. (A6), $\hat{\hat{c}}$ is the tensor of the elastic moduli. The corresponding twinning (stray) energy takes the form

$$F_{\mathrm{stray}} = \frac{1}{4\pi}\int_{\Omega} dV \int_{S} dS \frac{(\mathbf{N},\mathbf{r}-\mathbf{r}_S)}{|(\mathbf{r}-\mathbf{r}_S)|^3}\hat{u}^{(\mathrm{ms})}(\mathbf{r})\hat{\hat{c}}\hat{q}(\mathbf{r}_S). \qquad \text{(A7)}$$

The main contribution to the stray energy arises from the macrostresses related to a homogeneous part of the $\hat{u}^{(\mathrm{ms})}(\mathbf{r})$ strains, $\langle\hat{u}^{(\mathrm{ms})}(\mathbf{r})\rangle$, averaged over the layer volume.[28] For a *z*-oriented layer this gives rise to the expression

$$F_{\mathrm{stray}} = V\left\{\frac{1}{2}c_{11}[\langle u_{xx}^{(\mathrm{ms})}\rangle^2 + \langle u_{yy}^{(\mathrm{ms})}\rangle^2] + c_{12}\langle u_{xx}^{(\mathrm{ms})}\rangle\langle u_{yy}^{(\mathrm{ms})}\rangle + 2c_{44}\langle u_{xy}^{(\mathrm{ms})}\rangle^2\right\}. \qquad \text{(A8)}$$

Neglecting the isomorphic magnetostriction $u_{xx}^{(\mathrm{ms})} + u_{yy}^{(\mathrm{ms})}$ which does not contribute to the formation of domain structure, and with account of the crystal symmetry, Eq. (A8) gives rise to Eq. (4). It should be stressed that as in magnetism, the stray energy related to the averaged strains is proportional to the volume of the sample and thus cannot be neglected for any sample size.

[1] T. M. Giebultowicz, P. Klosowski, N. Samarth, H. Luo, and J. K. Furdyna, Phys. Rev. B **48**, 12 817 (1993).

[2] T. M. Giebultowicz, W. Faschinger, V. Nunez, P. Klosowski, G. Bauer, H. Sitter, and J. K. Furdyna, J. Cryst. Growth **138**, 877 (1994).

[3] W. Szuszkiewicz, B. Hennion, M. Jouanne, J. F. Morhange, E. Dynowska, E. Janik, and T. Wojtowicz, J. Magn. Magn. Mater. **196-197**, 425 (1999).

[4] V. Nunez, T. M. Giebultowicz, W. Faschinger, G. Bauer, H. Sitter, and J. K. Furdyna, J. Magn. Magn. Mater. **140-144**, 633 (1995).

[5] P. Klosowski, T. M. Giebultowicz, J. J. Rhyne, N. Samarth, H. Luo, and J. K. Furdyna, J. Appl. Phys. **70**, 6221 (1991).

[6] W. Szuszkiewicz, B. Hennion, E. Dynowska, E. Janik, T. Wojtowicz, and M. Zielinski, in Proceedings of XXVIII International School on the Physics of Semiconducting Compounds, Ustron-Jaszowiec, Poland, 1999, p. 101.

[7] J. J. Rhyne, J. Lin, J. K. Furdyna, and T. M. Giebultowicz, J. Magn. Magn. Mater. **177-181**, 1195 (1998).

[8] J. Lin, J. J. Rhyne, J. K. Furdyna, and T. M. Giebultowicz, J. Appl. Phys. **83**, 6554 (1998).

[9] W. Szuszkiewicz (private communication).

[10] L. E. Stumpe, J. J. Rhyne, H. Kaiser, S. Lee, U. Bindley, and J. K. Furdyna, J. Appl. Phys. **87**, 6460 (2000).

[11] N. Samarth, P. Klosowski, H. Luo, T. M. Giebultowicz, J. K. Furdyna, J. J. Rhyne, B. E. Larson, and N. Otsuka, Phys. Rev. B **44**, 4701 (1991).

[12] B. E. Larson, K. C. Hass, and H. Ehrenreich, Phys. Rev. B **37**, 4137 (1988).

[13] T. M. Giebultowicz, V. Nunez, G. Springholz, G. Bauer, J. Chen, M. S. Dresselhaus, and J. K. Furdyna, J. Appl. Phys. **76**, 6291 (1994).

[14] T. M. Giebultowicz, V. Nunez, G. Springholz, G. Bauer, J. Chen, M. S. Dresselhaus, and J. K. Furdyna, J. Magn. Magn. Mater. **140-144**, 635 (1995).

[15] H. Kepa, T. M. Giebultowicz, K. I. Goldman, V. Nunez, C. F. Majkrzak, G. Springholz, and G. Bauer, J. Appl. Phys. **81**, 5373 (1997).

[16] H. Kepa, K. I. Goldman, T. M. Giebultowicz, C. F. Majkrzak, G. Springholz, H. Krenn, S. Holl, F. Schinagl, and G. Bauer, Physica E (Amsterdam) **2**, 399 (1998).

[17] K. I. Goldman, G. Springholz, H. Kepa, T. M. Giebultowicz, C. F. Majkrzak, and G. Bauer, Physica B **241-243**, 710 (1998).

[18] Long-range ordering in two-dimensional AFM resulting from magnetoelastic interactions was described in Ref. 19.

[19] B. A. Ivanov and E. V. Tartakovskaya, Pis'ma Zh. Éksp. Teor. Fiz. **63**, 792 (1996) [JETP Lett. **63**, 835 (1996)].

[20] O. V. Kovalev, in *Representation of the Crystallographic Space Groups. Irreducible Representations, Induced Representations and Co-representations*, edited by H. T. Stokes and D.M. Hatch (GB Science, 1993), p. 390.

[21] This means that we need one full dislocation to match the homogeneously strained AFM layer with the nonstrained nonmagnetic one at length *R*.

[22] For a detailed description of the so-called "method of inclusions" see Ref. 23.

[23] A. G. Khachaturyan, *Theory of Structural Transformations in Solids* (Wiley, New York, 1983).

[24] J. M. Ziman, *Models of Disorder* (Cambridge University Press, Cambridge, England, 1979).

[25] M. P. Maheswaranathan, R. J. Sladek, and U. Debska, Phys. Rev. B **31**, 5212 (1985).

[26] T. M. Rusin, Phys. Rev. B **58**, 2107 (1998).

[27] C. Teodosiu, *Elastic Models of Crystal Defects* (Springer-Verlag, Berlin, 1982), p. 352.

[28] Microstresses related to the inhomogeneous part of $\hat{u}^{(\mathrm{ms})}$ are localized in the interface region according to the Saint-Venan principle; see, e.g., Ref. 29.

[29] A. L. Roitburd, J. Appl. Phys. **83**, 239 (1998).